Published in final edited form as:
J Immunol. 2010 October 15; 185(8): 4705–4713. doi:10.4049/jimmunol.1002276.

Negative selection and peptide chemistry determine the size of naïve foreign peptide-MHCII-specific CD4+ T cell populations

H. Hamlet Chu[*], **James J. Moon**[*,‡], **Andrew C. Kruse**[†], **Marion Pepper**[*], and **Marc K. Jenkins**[*]

[*]Department of Microbiology, Center for Immunology, University of Minnesota Medical School, Minneapolis, Minnesota, USA 55455

[†]Department of Biochemistry, University of Minnesota Medical School, Minneapolis, Minnesota, USA 55455

Abstract

Naïve CD4+ T cell populations that express TCRs specific for different foreign peptide-MHCII (pMHCII) ligands can vary in size over several orders of magnitude. This variation may explain why immune responses to some peptides are stronger than others. Here we used a sensitive pMHCII-tetramer based cell enrichment method to study the derivation of two naïve foreign pMHCII-specific naïve CD4+ T cell populations that differed in size by 8-fold in normal mice. Analysis of mice in which thymic negative selection was impaired revealed that the smaller population underwent more clonal deletion than the larger population. In addition, large naïve cell populations tended to recognize peptides with tryptophan residues as TCR contacts. Thus, the foreign pMHCII that tend to be recognized by large naïve populations induce minimal clonal deletion and contain certain amino acids with the capacity to interact favorably with TCRs.

Keywords

Repertoire; thymic selection; frequency; immunodominance

Introduction

T cells expressing αβ TCR recognize peptides embedded in MHC molecules (pMHC) displayed by APCs (1). Each TCR chain has a unique amino acid sequence generated by random rearrangement of V, (D), and J segments (2). Cells that express non-functional TCRs or TCRs with high affinity for self-pMHC are eliminated during development in the thymus. Survivors populate the secondary lymphoid organs and form a diverse repertoire of naïve T cells each expressing a unique TCR capable of binding a few of the several hundred thousand possible foreign-pMHC (2).

Recently, our laboratory and others directly measured the frequencies of different mouse and human foreign-pMHC-specific populations in the naïve repertoire and demonstrated that their sizes vary (3-9). For example, we found that C57BL/6 (B6) mice contained several hundred naïve CD4+ T cells specific for one peptide bound to the MHCII molecule of this

Address correspondence and reprint requests to Dr. Marc Jenkins, Department of Microbiology, Center for Immunology, Campus Code 2641, 2101 - 6th St. SE, Minneapolis, MN 55414. Telephone: 612-626-2715. jenki002@umn.edu.
‡Current address: Center for Immunology and Inflammatory Diseases, Pulmonary and Critical Care Unit, Massachusetts General Hospital and Harvard Medical School, Charlestown, MA 02129

Disclosures
The authors have no financial conflicts of interest.

strain (I-A^b) but only 20 cells specific for another (3, 7). Differences in naïve population size were found to account for the magnitude and TCR diversity observed in immune responses to different peptides. Therefore, the advantage provided by large naive population size could contribute to the phenomenon of immunodominance, although other variables such as the efficiency of pMHC generation (10) and the recruitment of naïve T cells into the response (8) are also important. Other studies showed that small naïve populations are at risk for extinction as the naïve T cell repertoire contracts during aging (11, 12).

The mechanism(s) that control the size of individual pMHC-specific populations in the naïve T cell repertoire are unknown. Thymic selection is one possibility. Developing thymocytes express randomly generated TCRs at the $CD4^+$ $CD8^+$ double positive stage of development (13). Only those cells expressing TCRs with low affinity for self-pMHC ligands displayed on the thymic cortical epithelium receive survival signals and are positively selected to become $CD4^+$ $CD8^-$ (CD4 SP) or $CD4^-$ $CD8^+$ (CD8 SP) mature T cells. Since multiple self-pMHC complexes can cause the positive selection of the same foreign-pMHC-specific population (14-16), it is possible that certain naïve populations are large because of a capacity to be positively selected by a large set of self-pMHC ligands. It is also possible that size differences between naïve pMHC-specific populations are caused by negative selection. For example, a foreign-pMHC-specific naive population may be small because many of its members are deleted due to high affinity cross reaction with a self-pMHC.

The structure of the pMHC might also influence the size of the corresponding naïve T cell population (17, 18). For example, Turner and colleagues found that influenza peptide-MHCI complexes with prominent TCR contact residues were recognized by larger and more diverse naïve $CD8^+$ T cell populations than less featured complexes (8, 19, 20). Similarly, we found that large naïve $CD4^+$ T populations contained more TCR Vβ chains than small populations (3), indicating that large population size was a consequence of pMHCII recognition by many diverse TCRs. Therefore, certain pMHC may have chemical features that allow binding by a wider range of TCRs than others.

Here we used a sensitive pMHCII-tetramer based cell enrichment method to assess the contributions of thymic selection and peptide composition to the derivation of two naïve foreign pMHCII-specific naïve $CD4^+$ T cell populations that differed in size by 8-fold in normal mice. The results indicate that the relative size of a given pMHCII-specific naïve $CD4^+$ T cell population is governed largely by negative selection and the chemical properties of the TCR-contacting amino acids in the peptide.

Materials and Methods

Mice

Six-8 week old C57BL/6 (B6) mice were purchased from the National Cancer Institute or The Jackson Laboratory. The *H2-DMa*$^{-/-}$, K14-A_b^b, *JH*$^{-/-}$, and μMT mice were kindly provided by A. Rudensky (Memorial Sloan-Kettering Cancer Center), T. Laufer (University of Pennsylvania), W. Weidanz (University of Wisconsin) and M. Farrar (University of Minnesota), respectively, and were bred in our facilities. All mice were housed under specific pathogen-free conditions in accordance with University of Minnesota and NIH guidelines.

Bone marrow chimeras

Lethally irradiated (1,000 rads) B6, *H2-DMa*$^{-/-}$ or Y-Ae mice were reconstituted with T-cell depleted bone marrow cells from B6, *H2-DMa*$^{-/-}$ or Y-Ae mice. Chimeras were used for experiments 7 to 8 weeks after bone marrow transfer.

Antibodies and peptides

Fluorochrome-labeled antibodies were purchased from eBioscience, Caltag, or BD PharMingen. All peptides were purchased from GenScript Corporation.

Immunization

Mice were injected intravenously with 50 μg of peptides with 5 μg of LPS (List Biologicals) and their spleens and lymph nodes were harvested at day 6 after injection.

2W:I-A^b model

The 2W:I-A^b model was prepared using Modeller 9v3 (Sali Lab, UCSF) to perform homology modeling with the template structure of I-A^b bound to the peptide 3K (PDB ID: 1LNU, (21)). Ten models were made and the one with the best Modeller score was selected for further optimization. The peptide portion of the best model was then further optimized with Modeller and inspected to verify that structural parameters (torsion angles, bond lengths, bond angles, etc.) fell within accepted limits. Repeating this procedure from the beginning several times showed that the Modeller predictions were highly similar in each case.

Plasmid construction

pRMHa-3 vectors containing the alpha and beta chains of I-A^b under the control of the metallothionein promoter were constructed as described in (3). Sequences encoding antigenic peptides (FliC 427-441: VQNRFNSAITNLGNT; $FliC_{1W}$: VQNRFWSAITNLGNT; $FliC_{2W}$: VQNRFWSAITNWGNT; 2W: EAWGALANWAVDSA; 3K: EAQKAKANKAVDKA; 1R: EARGALANWAVDSA; 1G: EAGGALANWAVDSA; 2G: EAGGALANGAVDSA; IgM heavy chain 376-391: EKYVTSAPMPEPGAPG, OVAC: HAAHAEINEAGC, $OVAC_{1W}$: HAWHAEINEAGC) were fused to the N-terminus of the I-A^b beta chain via a flexible polyglycine linker (22). All of the I-A^b beta chain constructs except for those containing OVAC and $OVAC_{1W}$ were co-transfected with the wild-type I-A^b alpha chain construct described by Moon et al. (3). I-A^b beta chain constructs containing OVAC or $OVAC_{1W}$ were co-transfected with an I-A^b alpha chain construct encoding a cysteine substitution at position 72. A disulfide bond between the substituted cysteine residue in the I-A^b alpha chain and the one just after the OVAC peptides formed in the transfected insect cells, in effect locking the peptide into the correct binding register (23-26).

pMHCII tetramer production

Peptide:I-A^b molecules were expressed in Drosophila S2 cells using the Drosophila Expression System kit (Invitrogen) as described by Moon et al. (3).

pMHCII tetramer-based enrichment

The protocol is described in detail in Moon et al. (3, 27). For TCR Vβ segment analysis, tetramer-enriched fractions from pooled mouse samples were split into multiple tubes and stained as described above with the addition of TCR Vβ-specific antibodies.

Peptide competition assay

The protocol was adapted from Ignatowicz et al. (28). In summary, spleen cells from *H2-DMa*$^{-/-}$ mice were incubated at 10^6 cells/ml in complete culture medium at 37°C for 8 hours with a limiting concentration (10 μg/ml) of $E\alpha_{52–66}$ peptide (ASFEAQGALANIAVDKA) (29) and various concentrations of the control $HA_{307-319}$ peptide or peptides of interest. The cells were then washed and stained with biotinylated anti-$E\alpha_{52–66}$:I-A^b (Y-Ae) (29, 30) at 4°C for 30 minutes. Cells were washed and then stained with streptavidin-conjugated PE

and anti-B220. Staining was measured on a LSRII (Becton Dickinson). Results were expressed as the Y-Ae median fluorescence intensity of the $B220^+$ cells measured in arbitrary units.

Statistical methods

Standard error of the mean and P-values were determined using Prism software (GraphPad Software, Inc.) with appropriate Student's t-test suggested by the program.

Results

Positive selection on a single self-pMHCII reduced the size of two foreign-pMHCII-specific naïve $CD4^+$ T cell populations

We studied naïve $CD4^+$ T cells specific for two different I-A^b-binding foreign peptides. One of the peptides called 2W (formerly 2W1S (3, 7, 21)) is a variant of peptide 52-68 from the I-Eα chain and contains the I-A^b binding nonamer core AWGALANWA. The other peptide comprised amino acids 427-441 from the FliC flagellar protein of *Salmonella enterica* serovar typhimurium (31) and contains the I-A^b binding nonamer core FNSAITNLG. Previously, we produced tetramers and used them with pMHCII tetramer-based cell enrichment method to show that individual B6 mice contain about 200-300 2W:I-A^b- and 25 FliC:I-A^b-binding naïve $CD4^+$ T cells in the spleen and lymph nodes (3, 7).

We reasoned that the 2W:I-A^b-specific population might be relatively large because of positive selection by multiple self-pMHCII. If so, then some cells in the 2W:I-A^b-specific population might be positively selected by a single self-pMHCII. A radiation bone marrow chimera-based approach was used to test this proposition. B6 bone marrow cells were injected into lethally irradiated *H2-DMa*$^{-/-}$ mice (32-34) or Y-Ae (35) single peptide (1P) mice. The radio-resistant thymic epithelial cells in these B6 > 1P chimeras predominantly expressed either CLiP:I-A^b or Eα:I-A^b, while B6 bone marrow-derived thymic dendritic cells displayed a diverse set of self-pMHCII. Since positive selection of a normal diverse $CD4^+$ T cell repertoire is based on diverse self-pMHCII display by cortical epithelial cells (36-38), only a limited set of $CD4^+$ T cells undergoes positive selection in B6 > 1P chimeric mice. In addition, since negative selection depends largely on diverse self-pMHCII display by medullary epithelial cells and bone marrow derived cells (39), the limited $CD4^+$ T cell repertoire in B6 > 1P mice is culled further by normal negative selection on the diverse set of self-pMHCII molecules displayed by B6 bone marrow derived cells (40, 41). In sum, the repertoire of $CD4^+$ T cells in a B6 > 1P chimeric mouse is the product of limited positive selection and normal negative selection.

Dual tetramer-based cell enrichment was then performed on thymocytes from individual B6 > 1P chimeras or normal B6 mice as controls. The CD4 SP population in normal B6 mice contained mutually exclusive naïve populations that bound the 2W:I-A^b or FliC:I-A^b tetramers (Fig. 1A). In contrast, 2W:I-A^b- or FliC:I-A^b-binding cells were not detected in the CD8 SP population in most B6 mice, and no mouse contained more than 5 such cells (Fig. 1A and B). This finding demonstrated that tetramer binding was TCR-specific since $CD4^+$ but not $CD8^+$ T cells bind to pMHCII ligands via the TCR (42). B6 mice had an average of 164 2W:I-A^b- and 19 FliC:I-A^b-specific CD4 SP cells per mouse (Fig. 1B). These values were significantly different from each other and both were significantly greater than the number of CD8 SP cells that bound each tetramer non-specifically. In contrast, B6 > 1P chimeric mice had an average of only 9 2W:I-A^b- and <5 FliC:I-A^b-specific CD4 SP cells per mouse (Fig. 1B). The value for 2W:I-A^b-but not FliC:I-A^b-specific cells was significantly, but barely above the background number of CD8 SP cells that bound tetramer non-specifically. Therefore, the positive selection of both 2W:I-A^b- and FliC:I-A^b-specific

$CD4^+$ T cells was heavily dependent on self-pMHCII other than CLiP:I-A^b or Eα:I-A^b. The observation that a few 2W:I-A^b-specific $CD4^+$ T cells could be positively selected by single self-pMHCII was consistent with the idea that a positive selection advantage may contribute to the large size of this population in normal mice.

Impairment of negative selection increased the size of two foreign-pMHCII-specific naïve $CD4^+$ T cell populations

It was also possible that thymic negative selection on self-pMHCII accounted for the difference in the size of 2W:I-A^b- and FliC:I-A^b-specific $CD4^+$ naïve T cell populations. Before assessing this possibility, we first confirmed that the pMHCII tetramer-based enrichment method had the sensitivity to detect clonal deletion of T cells specific for a genuine self-pMHCII. The peptide in the tetramer used for this purpose consisted of amino acids 376-391 from the IgM heavy chain constant region, which was identified by Rudensky and colleagues as an abundant I-A^b-bound self-peptide in B6 mice (43). An IgM:I-A^b tetramer was generated and used to enumerate IgM:I-A^b-specific T cells. Individual thymii from B6 mice contained an average of 6 IgM:I-A^{b+} $CD4^+$ $CD8^-$ cells (Fig 2A and B), which was at the detection limit of the enrichment method. In contrast, mice lacking B cells (μMT or $JH^{-/-}$ mice) contained an average of 45 IgM:I-A^{b+} $CD4^+$ $CD8^-$ cells per thymus (Fig 2A and B), which was significantly greater than the number of cells in B6 mice. Clonal deletion was a likely explanation for the presence of IgM:I-A^{b+} cells in B cell-deficient mice, but not B6 mice.

We next enumerated pMHCII-specific populations in K14-A_β^b mice in which negative selection was impaired. These mice express A_β^b molecules under the control of the *Krt14* promoter on the $A_\beta^{b-/-}$ background, which leads to I-A^b molecule expression on cortical epithelial cells but not medullary epithelial cells or bone marrow derived cells. Since positive selection depends on MHCII expression by cortical epithelial cells (36-38), this process occurs relatively normally in K14-A_β^b mice to produce a diverse repertoire of $CD4^+$ T cells. However, since negative selection depends largely on MHCII expression by medullary epithelial cells and bone marrow derived cells (39), the $CD4^+$ T cell repertoire in K14-A_β^b mice is not culled by this process and is thereby enriched for self-pMHCII-specific cells (40, 41).

Strikingly, the number of IgM:I-A^{b+} CD4 SP thymocytes was at least 50-fold higher in K14-A_β^b mice than in B6 or B cell-deficient mice (Fig. 2A and B). The finding that more IgM:I-A^{b+} CD4 SP thymocytes were present in K14-A_β^b mice than in B cell-deficient mice suggested that the pre-deletion repertoire of a normal B6 mouse contains thymocytes with high affinity for IgM:I-A^b alone, which appear in IgM-deficient mice, and a much larger population with high affinity for IgM:I-A^b and another self-pMHCII, which appear in K14-A_β^b mice. The presence of a few cells in K14-A_β^b mice that bound to IgM:I-A^b and 2W:I-A^b (Fig. 2A) provided further evidence that cross-reactive T cells were enriched in the pre-deletion repertoire.

This cross-reactivity raised the possibility that some cells specific for 2W:I-A^b or FliC:I-A^b might also be deleted in B6 mice due to cross-reactivity on unknown self-pMHCII. It was possible that more deletion of this type occurred in the FliC:I-A^b-specific population, explaining why it ends up smaller than the 2W:I-A^b-specific population. If this were the case, then the populations in K14-A_β^b mice would be expected to contain more cells and be similar in size. As shown in Fig. 2C, the number of 2W:I-A^b-specific cells increased from an average of 164 cells in B6 mice to 1,694 cells, while the number of FliC:I-A^b-specific cells increased from 19 cells to about 584 cells in K14-A_β^b mice. If it is assumed that K14-A_β^b mice contain the total pre-deletion repertoire, then the difference between the number of cells with a given pMHCII specificity in K14-A_β^b mice and B6 mice should equal the

number of cells that undergo clonal deletion in B6 mice. Thus, about 1,530 (1,694-164) or 90% of the potential 1,694 2W:I-A^b-specific cells that can develop in B6 mice normally undergo clonal deletion, while 565 (584-19) or 97% of the potential 584 FliC:I-A^b-specific cells had this fate. This analysis therefore supports the conclusion that the FliC:I-A^b-specific population experiences more negative selection than the 2W:I-A^b-specific population. About 300 of the cells in K14-$A_\beta{}^b$ mice that bound to 2W:I-A^b also bound to FliC:I-A^b, (Fig. 2D and E), indicating a high degree of pMHCII cross-reactivity by the cells in this population. Similar cells could not be found in B6 mice (Fig. 2D and E). This result indicates that the cells that are spared from negative selection in K14-$A_\beta{}^b$ mice can recognize multiple self-pMHCII. This cross-reactivity probably explains why K14-$A_\beta{}^b$ mice contained more 2W:I-A^b- and FliC:I-A^b-specific cells than B6 mice but had the same number of total $CD4^+$ T cells (Fig. 2F).

One explanation for the greater sensitivity of the FliC:I-A^b-specific population to negative selection was that the TCRs on more of its constituents were promiscuous with respect to self-pMHCII recognition. In this case, the FliC:I-A^b-specific population would be more likely than the 2W:I-A^b-specific population to undergo negative selection in response to any single self-pMHCII ligand. This possibility was tested in 1P > B6 chimeric mice in which negative selection was induced by CLiP:I-A^b or Eα:I-A^b complexes on bone marrow-derived cells, in the presence of normal positive selection by diverse self-pMHCII ligands on thymic epithelial cells. As shown in Fig. 2C, the number of 2W:I-A^b-specific cells increased from an average of 164 cells in B6 mice to 878 cells, while the number of FliC:I-A^b-specific cells increased 19 cells to 68 cells in 1P > B6 chimeric mice. Again, based on the assumption that K14-$A_\beta{}^b$ mice contain the total pre-deletion repertoire, these results indicate that 48% ({1,694-878/1,694}*100) of the 2W:I-A^b- and 88% ({584-68/584}*100) of the FliC:I-A^b-specific cells that could develop in B6 mice were deleted in 1P > B6 chimeric mice. These results therefore support the conclusion that a wider range of self-pMHCII ligands can cause negative selection in the FliC:I-A^b-specific population than the 2W:I-A^b-specific population.

The large size of the 2W:I-A^b-specific population is associated with specific TCR contact residues in the peptide

Although differential negative selection was a determining factor, it was not the only factor since the 2W:I-A^b-specific population was still 3-fold larger than the FliC:I-A^b-specific population in the absence of negative selection (Fig. 2C). We therefore explored a chemical explanation for the capacity of the 2W peptide to be recognized by a large naïve population by comparing it to a closely related peptide called 3K (21, 44). The 3K and 2W peptides differ at TCR contact amino acids at positions P2, P3, P5 and P8 but are identical at the I-A^b anchor amino acids at the other positions (Fig. 3A). The population of 3K:I-A^b-specific naïve $CD4^+$ T cell in the spleen and lymph nodes or thymus was about 8-fold smaller than the 2W:I-A^b-specific population (Fig. 3B and C). This result suggested that the capacity of 2W:I-A^b to be bound by a larger naïve population than 3K:I-A^b was due to its TCR contact residues.

To visualize the topology of the TCR contact residues of these pMHCII complexes, the 2W:I-A^b complex was modeled on the known crystal structure of 3K:I-A^b (PDB ID: 1LNU, (44)) (Fig. 3D). This modeling revealed that the side chains from the tryptophan residues at P2 and P8 of the 2W peptide protrude from the solvent exposed surface of I-A^b and are thus likely to contribute significantly to TCR binding (Fig. 3D). In contrast, the glycine at P3 and the leucine at P5 are less likely to contribute to this surface because the glycine does not extend above the peptide-binding groove and the leucine residue is partially occluded by a glutamic acid residue in the β1-helix of the I-A^b molecule (Fig. 3D). Thus, this analysis suggested that the P2 and P8 tryptophans were the most important TCR contacts in 2W:I-A^b

We produced several 2W variant peptides in which the tryptophan residues at position P2 were changed to glycine (1G) or arginine (1R) or the tryptophan residues at positions P2 and P8 were both changed to glycine (2G) to test for the role of these positions in the large size of the 2W:I-A^b-specific population (Fig. 4A). These substitutions were chosen because glycine lacks a side chain and therefore offers minimal possibilities for engaging in favorable binding interactions with the TCR, while arginine is capable of engaging in charge-charge interactions and hydrogen bonding through its guanidinium group as well as hydrophobic interactions with the rest of its side chain. Each of the substituted peptides but not an irrelevant peptide had the same capacity as the 2W peptide to compete with a reference peptide for binding to I-A^b (Fig. 4B).

I-A^b tetramers containing the variant 2W peptides were produced and used to enumerate the corresponding naïve $CD4^+$ T cell populations. As shown in Fig. 4C, defined populations of naïve $CD4^+$ T cells specific for each of the three variant 2W:I-A^b complexes were detected in B6 mice. Eighty-five to 95% of the naïve $CD4^+$ T cells identified by each of the variant 2W:I-A^b tetramers failed to bind the 2W:I-A^b tetramer as expected because changes were made in TCR contacts. Importantly, the $CD4^+$ T cell populations specific for the 1G and 1R variants were 3-fold smaller (127 ± 39 and 108 ± 36, respectively) than the 2W:I-A^b-specific population, while the population specific for the 2G variant was 6 times smaller (62 ± 13) (Fig. 4D. This basic hierarchy (2W > 1G = 1R > 2G) was also observed for expanded populations present 6 days after intravenous injection of 50 μg of the relevant peptide plus LPS as an adjuvant (Fig. 5A), although the expanded 2G:I-A^b-specific population was even smaller than predicted by its naive frequency. Collectively, these results are consistent with the hypothesis that the tryptophan TCR contact residues in the 2W peptide contributed to the large size of the 2W:I-A^b-specific T cell population. In addition, tryptophan was superior to arginine in this regard despite the potentially favorable properties of the latter amino acid.

We next tested the hypothesis that the 2W:I-A^b-specific population was larger than those specific for the variant 2W:I-A^b ligands because of recognition by more TCRs. The TCR Vβ chain usage of 2W:I-A^b- and 1G:I-A^b-specific populations was examined in B6 mice immunized with the relevant peptides. As reported previously (3), the 2W:I-A^b-specific population consisted of T cells that utilized all 14 TCR Vβ chains tested. On the contrary, T cells using Vβ5.1/5.2, Vβ9, Vβ10b, or Vβ11 chains were absent in the 1G:I-A^b-specific population, while the percentage of Vβ2, Vβ8.3, and Vβ12-expressing T cells was twice that of the 2W:I-A^b-specific population (Fig. 5B). Taken together, these results suggested that 2W:I-A^b was recognized by more diverse TCRs than 1G:I-A^b.

Tryptophan residues at TCR contact P2 and P8 increase the size of other peptide:I-A^b-specific naïve T cell populations

The results suggested that the presence of tryptophan as a TCR contact residue at P2 of the 2W peptide allowed recognition by more TCRs. If this was correct, then substitution with tryptophan at P2 of peptides that are normally recognized by small naïve T cell populations should result in a pMHCII that is recognized by a larger naïve population. To test this hypothesis, we first generated two tetramers containing variants of the FliC peptide with tryptophan substitutions at P2 alone ($FliC_{1W}$) or P2 and P8 ($FliC_{2W}$) (Fig 6A). These FliC variant peptides had the same I-A^b binding efficiency as the FliC parent peptide (Fig 6B) and produced stable I-A^b tetramers. The $FliC_{1W}$:I-A^b and $FliC_{2W}$:I-A^b tetramers detected 2-fold and 4-fold more naïve CD4+ T cells in the spleen and lymph nodes of B6 mice, respectively, than were detected by the FliC:I-A^b tetramer (Fig. 6C). These tetramer binding populations were mutually exclusive (data not shown), indicating that the tryptophan residues in P2 and P8 positions altered the topology of complexes such that the variant FliC:I-A^b tetramers bound to a completely different yet larger set of T cells.

To rule out the possibility that these results occurred by chance, the tryptophan substitution experiment was performed with a different peptide. The chicken OVA peptide 329-337 was chosen for this purpose. This is a well-studied peptide recognized by $CD4^+$ T cells from the OT-II TCR transgenic line (23, 45). Tetramers containing $OVA_{329\text{-}337}$ (OVAC) or $OVA_{329\text{-}337}$ with a tryptophan substitution at P2 ($OVAC_{1W}$) were produced and used to detect naive $CD4^+$ T cells. The $OVAC_{1W}$:I-A^b tetramer detected an average of 100 naïve $CD4^+$ T cells that was about 2.5-times larger than the population detected by the OVAC:I-A^b tetramer (Fig. 6D). These results confirm those obtained with the FliC:I-A^b tetramers and solidify the conclusion that the presence of a tryptophan residue at P2 of an I-A^b-binding peptide produces a complex that can be recognized by a relatively large naïve T cell population.

Discussion

We sought to determine if differences in thymic selection could be the explanation for variation in naïve pMHCII-specific $CD4^+$ T cell population size. To do so, it was necessary to detect the relevant naïve pMHCII-specific CD4 SP cells in the thymus. The results indicate that the pMHCII tetramer-based cell enrichment method is sensitive enough for this purpose. Interestingly, the number of 2W:I-A^b- or FliC:I-A^b-specific CD4 SP thymocytes was within 2-fold of the number of naïve T cells of these specificities in the secondary lymphoid organs (3). The relatively large number of pMHCII-specific thymocytes relative to peripheral naïve cells is surprising given the high rate of export of naïve cells from the thymus (46) and the long half-life of naïve T cells in the secondary lymphoid organs (47). The current results indicated that some of the CD4 SP thymocytes do not enter the peripheral pool, or some of the peripheral naïve cells turn over at a higher than expected rate.

The finding that almost no 2W:I-A^b- or FliC:I-A^b-specific $CD4^+$ T cells developed when positive selection was limited to a either CLiP:I-A^b or Eα:I-A^b showed that most cells in both populations required self peptide:I-A^b ligands other than these for positive selection. However, a few 2W:I-A^b-but not FliC:I-A^b-specific naïve T cells could be selected on single self-pMHCII ligands suggesting that an advantage in positive selection efficiency might contribute to the relatively large size of the former population. However, it was difficult to reach a firm conclusion on this point because so few cells of either specificity developed under conditions of limited positive selection.

Our results provided clearer evidence that negative selection is an important factor in the size of a given naïve $CD4^+$ T cell population. Not surprisingly, the effect of negative selection was clearly seen in the analysis of a genuine self pMHCII-specific population. IgM:I-A^b-specific T cells went from being undetectable in B6 mice to a population of several thousand cells in K14-$A_\beta{}^b$ mice, in which clonal deletion is greatly impaired.

More remarkable was the extent to which the number of foreign pMHCII-specific T cells was influenced by negative selection. Comparison of B6 and K14-$A_\beta{}^b$ mice revealed that a large number of 2W:I-A^b- and FliC:I-A^b-specific T cells are generated by positive selection, only to be deleted. This deletion is likely a consequence of avid cross-reaction on unknown self-pMHCII displayed by bone marrow-derived cells. The broad cross-reactivity of the "should have been deleted" population was revealed by the finding that some cells in K14-$A_\beta{}^b$ mice bound to 2W:I-A^b *and* IgM:I-A^b or 2W:I-A^b *and* FliC:I-A^b. Importantly, the pre-deletion repertoire of FliC:I-A^b-specific cells appeared to contain more of these cross-reactive cells than the 2W:I-A^b-specific repertoire. This contention is based on the observation that the number of FliC:I-A^b-specific cells in B6 mice was 3% of that in K14-$A_\beta{}^b$ mice, while it was 10% for 2W:I-A^b-specific cells. This difference correlated with the

observation that 2 randomly chosen single pI-A^b ligands caused deletion of a much larger fraction of the pre-deletion repertoire of FliC:I-A^b-specific cells than of the 2W:I-A^b-specific repertoire. Together, these results suggest that the smallness of the FliC:I-A^b-specific population in B6 mice is due in part to fact that the pre-deletion population from which it is derived contains very few cells that can avidly recognize FliC:I-A^b but no other self-peptide-I-A^b complexes. In contrast, the pre-deletion population of 2W:I-A^b-specific cells appears to contain many more cells that can avidly recognize 2W:I-A^b but no other self-peptide-I-A^b complexes and thus survive deletion.

The finding that some of the cells that were spared from deletion in K14-A_β^b mice could bind to both 2W:I-A^b and IgM:I-A^b or FliC:I-A^b is consistent with other work showing that pMHCII-specific T cells that develop in the presence of reduced negative selection are degenerate with respect to peptide specificity (48, 49). This phenomenon may have relevance to control of infection. It has recently been proposed that HLA-B57 MHCI molecules bind fewer distinct self-peptides than other human MHCI molecules, and thus impose less stringent negative selection (49). This property correlated with the observation that HIV-infected humans who express HLA-B57 contain more HIV peptide-specific $CD8^+$ T cells that cross-react on variants of the relevant peptide and control HIV infection better than individuals who express other HLA alleles. This advantage may relate to HLA-B57-restricted T cells being more cross-reactive and capable of retaining reactivity to variant peptides created by viral mutation. It would of interest to use the pMHC enrichment method described here to determine whether HIV peptide:HLA-B57-specific $CD8^+$ are more numerous and cross-reactive than other pMHCI-specific populations in naïve individuals.

Despite the clear role of negative selection in controlling the absolute number of pMHC-specific T cells, perturbation of this process did not change the fact that the 2W:I-A^b-specific population was still larger than the FliC:I-A^b-specific one in the absence of negative selection. Rather, our study suggests that this phenomenon is related to the specific amino acids present at P2 and P8 of these peptides. In most cases, individual weak interactions between TCR loops and the side chains of amino acids at P2, P3, P5, and P8 of the peptide each contribute to the total binding energy of a TCR to its cognate pMHC (48, 49). Our results suggest that tryptophan residues at P2 and P8 create a particularly favorable binding surface for many TCRs, which could explain why the 2W:I-A^b-specific population is relatively large. This capacity could be related to the ability of the indole ring of tryptophan to form hydrogen bonds, hydrophobic, and cation-pi stacking interactions with a variety of other amino acids (50, 51). However, the finding that the 2W:I-A^b-specific population was still larger than the $FliC_{2W}$:I-A^b-specific population, despite the presence of tryptophan residues at P2 and P8 in both peptides suggests that other factors contribute to this difference. It is possible that the leucine at P5 of the 2W peptide may also enhance TCR binding, although it is mostly hidden behind an amino acid from the I-A^b beta chain. Alternatively, the P5 amino acid or residues flanking the nonamer core of the $FliC_{2W}$ peptide may have adverse effects on TCR binding. A comprehensive mutagenesis study of all TCR contact residues in the 2W peptide will be necessary to address these possibilities.

Turner and colleagues also identified a correlation between the structure of foreign pMHCI ligands and the size of the complementary $CD8^+$ T cell populations (19). These investigators compared the repertoires specific for influenza peptide $PA_{224-236}$ or NP_{366-74} bound to H-2D^b (52). The NP_{366-74}:D^b complex contains less featured TCR contact residues than the $PA_{224-236}$:D^b complex and was found to be recognized by a smaller and less diverse naïve T cell population (8). Similarly, we found that the 2W:I-A^b-specific naïve population had a more diverse TCR repertoire than the smaller 1G:I-A^b- and FliC:I-A^b-specific (3) populations. These results suggest that an understanding of the rules that favor peptide side chain-TCR interaction could allow prediction of not only which peptides have properly

spaced MHC anchor residues but also TCR contact residues that are likely to be recognized by relatively large naïve T cell populations. This knowledge could make it possible to identify potential immunodominant peptides from pathogens using bioinformatic approaches.

Acknowledgments

We thank D. Ohlendorf for advice on generating the 2W:I-A^b model; P. Allen (Washington University) and J. Kappler (HHMI and National Jewish Medical Research Center) for suggesting the disulfide trap strategy for OVA:I-A^b tetramer production; K. Hogquist and S. Jameson for comments on the manuscript.

This work was supported by the American Heart Association Predoctoral Fellowship (to H.H.C.), and National Institutes of Health Grant R01 AI39614 and R37 AI27998 (to M.K.J.).

Abbreviation used in this paper

B6	C57BL/6
CD4 SP	$CD4^+$ $CD8^-$ thymocyte
CD8 SP	$CD4^-$ CD8+ thymocyte
1P	single peptide
MFI	mean fluorescence intensity
pMHCII	peptide-MHCII complex

References

1. Rudolph MG, Stanfield RL, Wilson IA. How TCRs bind MHCs, peptides, and coreceptors. Annu. Rev. Immunol. 2006; 24:419–466. [PubMed: 16551255]
2. Davis MM, Bjorkman PJ. T-cell antigen receptor genes and T-cell recognition. Nature. 1988; 334:395–402. [PubMed: 3043226]
3. Moon JJ, Chu HH, Pepper M, McSorley SJ, Jameson SC, Kedl RM, Jenkins MK. Naive CD4(+) T cell frequency varies for different epitopes and predicts repertoire diversity and response magnitude. Immunity. 2007; 27:203–213. [PubMed: 17707129]
4. Obar JJ, Khanna KM, Lefrancois L. Endogenous naive CD8+ T cell precursor frequency regulates primary and memory responses to infection. Immunity. 2008; 28:859–869. [PubMed: 18499487]
5. Kotturi MF, Scott I, Wolfe T, Peters B, Sidney J, Cheroutre H, von Herrath MG, Buchmeier MJ, Grey H, Sette A. Naive precursor frequencies and MHC binding rather than the degree of epitope diversity shape CD8+ T cell immunodominance. J. Immunol. 2008; 181:2124–2133. [PubMed: 18641351]
6. Haluszczak C, Akue AD, Hamilton SE, Johnson LD, Pujanauski L, Teodorovic L, Jameson SC, Kedl RM. The antigen-specific CD8+ T cell repertoire in unimmunized mice includes memory phenotype cells bearing markers of homeostatic expansion. J. Exp. Med. 2009; 206:435–448. [PubMed: 19188498]
7. Chu HH, Moon JJ, Takada K, Pepper M, Molitor JA, Schacker TW, Hogquist KA, Jameson SC, Jenkins MK. Positive selection optimizes the number and function of MHCII-restricted CD4+ T cell clones in the naive polyclonal repertoire. Proc. Natl. Acad. Sci. U S A. 2009; 106:11241–11245. [PubMed: 19541603]
8. La Gruta NL, Rothwell WT, Cukalac T, Swan NG, Valkenburg SA, Kedzierska K, Thomas PG, Doherty PC, Turner SJ. Primary CTL response magnitude in mice is determined by the extent of naive T cell recruitment and subsequent clonal expansion. J. Clin. Invest. 2010; 120:1885–1894. [PubMed: 20440073]
9. Legoux F, Debeaupuis E, Echasserieau K, De La Salle H, Saulquin X, Bonneville M. Impact of TCR reactivity and HLA phenotype on naive CD8 T cell frequency in humans. J. Immunol. 2010; 184:6731–6738. [PubMed: 20483723]

10. Yewdell JW. Confronting complexity: real-world immunodominance in antiviral CD8+ T cell responses. Immunity. 2006; 25:533–543. [PubMed: 17046682]
11. Yager EJ, Ahmed M, Lanzer K, Randall TD, Woodland DL, Blackman MA. Age-associated decline in T cell repertoire diversity leads to holes in the repertoire and impaired immunity to influenza virus. J. Exp. Med. 2008; 205:711–723. [PubMed: 18332179]
12. Ahmed M, Lanzer KG, Yager EJ, Adams PS, Johnson LL, Blackman MA. Clonal expansions and loss of receptor diversity in the naive CD8 T cell repertoire of aged mice. J. Immunol. 2009; 182:784–792. [PubMed: 19124721]
13. Starr TK, Jameson SC, Hogquist KA. Positive and negative selection of T cells. Annu. Rev. Immunol. 2003; 21:139–176. [PubMed: 12414722]
14. Hogquist KA, Tomlinson AJ, Kieper WC, McGargill MA, Hart MC, Naylor S, Jameson SC. Identification of a naturally occurring ligand for thymic positive selection. Immunity. 1997; 6:389–399. [PubMed: 9133418]
15. Lo WL, Felix NJ, Walters JJ, Rohrs H, Gross ML, Allen PM. An endogenous peptide positively selects and augments the activation and survival of peripheral CD4+ T cells. Nat. Immunol. 2009; 10:1155–1161. [PubMed: 19801984]
16. Ebert PJ, Jiang S, Xie J, Li QJ, Davis MM. An endogenous positively selecting peptide enhances mature T cell responses and becomes an autoantigen in the absence of microRNA miR-181a. Nat. Immunol. 2009; 10:1162–1169. [PubMed: 19801983]
17. Meijers R, Lai CC, Yang Y, Liu JH, Zhong W, Wang JH, Reinherz EL. Crystal structures of murine MHC Class I H-2 D(b) and K(b) molecules in complex with CTL epitopes from influenza A virus: implications for TCR repertoire selection and immunodominance. J. Mol. Biol. 2005; 345:1099–1110. [PubMed: 15644207]
18. Stewart-Jones GB, McMichael AJ, Bell JI, Stuart DI, Jones EY. A structural basis for immunodominant human T cell receptor recognition. Nat. Immunol. 2003; 4:657–663. [PubMed: 12796775]
19. Turner SJ, Kedzierska K, Komodromou H, La Gruta NL, Dunstone MA, Webb AI, Webby R, Walden H, Xie W, McCluskey J, Purcell AW, Rossjohn J, Doherty PC. Lack of prominent peptide-major histocompatibility complex features limits repertoire diversity in virus-specific CD8+ T cell populations. Nat. Immunol. 2005; 6:382–389. [PubMed: 15735650]
20. Kedzierska K, Guillonneau C, Gras S, Hatton LA, Webby R, Purcell AW, Rossjohn J, Doherty PC, Turner SJ. Complete modification of TCR specificity and repertoire selection does not perturb a CD8+ T cell immunodominance hierarchy. Proc. Natl. Acad. Sci. U S A. 2008; 105:19408–19413. [PubMed: 19047637]
21. Rees W, Bender J, Teague TK, Kedl RM, Crawford F, Marrack P, Kappler J. An inverse relationship between T cell receptor affinity and antigen dose during CD4(+) T cell responses in vivo and in vitro. Proc. Natl. Acad. Sci. U S A. 1999; 96:9781–9786. [PubMed: 10449771]
22. Kozono H, White J, Clements J, Marrack P, Kappler J. Production of soluble MHC class II proteins with covalently bound single peptides. Nature. 1994; 369:151–154. [PubMed: 8177320]
23. Robertson JM, Jensen PE, Evavold BD. DO11.10 and OT-II T cells recognize a C-terminal ovalbumin 323-339 epitope. J. Immunol. 2000; 164:4706–4712. [PubMed: 10779776]
24. Landais E, Romagnoli PA, Corper AL, Shires J, Altman JD, Wilson IA, Garcia KC, Teyton L. New design of MHC class II tetramers to accommodate fundamental principles of antigen presentation. J. Immunol. 2009; 183:7949–7957. [PubMed: 19923463]
25. Truscott SM, Lybarger L, Martinko JM, Mitaksov VE, Kranz DM, Connolly JM, Fremont DH, Hansen TH. Disulfide bond engineering to trap peptides in the MHC class I binding groove. J. Immunol. 2007; 178:6280–6289. [PubMed: 17475856]
26. Stadinski BD, Zhang L, Crawford F, Marrack P, Eisenbarth GS, Kappler JW. Diabetogenic T cells recognize insulin bound to IAg7 in an unexpected, weakly binding register. Proc. Natl. Acad. Sci. U S A. 2010; 107:10978–10983. [PubMed: 20534455]
27. Moon JJ, Chu HH, Hataye J, Pagan AJ, Pepper M, McLachlan JB, Zell T, Jenkins MK. Tracking epitope-specific T cells. Nat. Protoc. 2009; 4:565–581. [PubMed: 19373228]

28. Ignatowicz L, Rees W, Pacholczyk R, Ignatowicz H, Kushnir E, Kappler J, Marrack P. T cells can be activated by peptides that are unrelated in sequence to their selecting peptide. Immunity. 1997; 7:179–186. [PubMed: 9285403]
29. Murphy DB, Lo D, Rath S, Brinster RL, Flavell RA, Slanetz A, Janeway CA Jr. A novel MHC class II epitope expressed in thymic medulla but not cortex. Nature. 1989; 338:765–768. [PubMed: 2469959]
30. Rudensky A, Rath S, Preston-Hurlburt P, Murphy DB, Janeway CA Jr. On the complexity of self. Nature. 1991; 353:660–662. [PubMed: 1656278]
31. McSorley SJ, Cookson BT, Jenkins MK. Characterization of CD4+ T cell responses during natural infection with Salmonella typhimurium. J. Immunol. 2000; 164:986–993. [PubMed: 10623848]
32. Fung-Leung WP, Surh CD, Liljedahl M, Pang J, Leturcq D, Peterson PA, Webb SR, Karlsson L. Antigen presentation and T cell development in H2-M-deficient mice. Science. 1996; 271:1278–1281. [PubMed: 8638109]
33. Miyazaki T, Wolf P, Tourne S, Waltzinger C, Dierich A, Barois N, Ploegh H, Benoist C, Mathis D. Mice lacking H2-M complexes, enigmatic elements of the MHC class II peptide-loading pathway. Cell. 1996; 84:531–541. [PubMed: 8598040]
34. Martin WD, Hicks GG, Mendiratta SK, Leva HI, Ruley HE, Van Kaer L. H2-M mutant mice are defective in the peptide loading of class II molecules, antigen presentation, and T cell repertoire selection. Cell. 1996; 84:543–550. [PubMed: 8598041]
35. Ignatowicz L, Kappler J, Marrack P. The repertoire of T cells shaped by a single MHC/peptide ligand. Cell. 1996; 84:521–529. [PubMed: 8598039]
36. Bill J, Palmer E. Positive selection of CD4+ T cells mediated by MHC class II-bearing stromal cell in the thymic cortex. Nature. 1989; 341:649–651. [PubMed: 2571938]
37. Vukmanovic S, Grandea AG 3rd, Faas SJ, Knowles BB, Bevan MJ. Positive selection of T-lymphocytes induced by intrathymic injection of a thymic epithelial cell line. Nature. 1992; 359:729–732. [PubMed: 1331804]
38. Markowitz JS, Auchincloss H Jr. Grusby MJ, Glimcher LH. Class II-positive hematopoietic cells cannot mediate positive selection of CD4+ T lymphocytes in class II-deficient mice. Proc. Natl. Acad. Sci. U S A. 1993; 90:2779–2783. [PubMed: 8464889]
39. Hogquist KA, Baldwin TA, Jameson SC. Central tolerance: learning self-control in the thymus. Nat. Rev. Immunol. 2005; 5:772–782. [PubMed: 16200080]
40. Laufer TM, DeKoning J, Markowitz JS, Lo D, Glimcher LH. Unopposed positive selection and autoreactivity in mice expressing class II MHC only on thymic cortex. Nature. 1996; 383:81–85. [PubMed: 8779719]
41. Laufer TM, Fan L, Glimcher LH. Self-reactive T cells selected on thymic cortical epithelium are polyclonal and are pathogenic in vivo. J. Immunol. 1999; 162:5078–5084. [PubMed: 10227976]
42. Singer A, Bosselut R. CD4/CD8 coreceptors in thymocyte development, selection, and lineage commitment: analysis of the CD4/CD8 lineage decision. Adv. Immunol. 2004; 83:91–131. [PubMed: 15135629]
43. Dongre AR, Kovats S, deRoos P, McCormack AL, Nakagawa T, Paharkova-Vatchkova V, Eng J, Caldwell H, Yates JR 3rd, Rudensky AY. In vivo MHC class II presentation of cytosolic proteins revealed by rapid automated tandem mass spectrometry and functional analyses. Eur. J. Immunol. 2001; 31:1485–1494. [PubMed: 11465105]
44. Liu X, Dai S, Crawford F, Fruge R, Marrack P, Kappler J. Alternate interactions define the binding of peptides to the MHC molecule IA(b). Proc. Natl. Acad. Sci. U S A. 2002; 99:8820–8825. [PubMed: 12084926]
45. Barnden MJ, Allison J, Heath WR, Carbone FR. Defective TCR expression in transgenic mice constructed using cDNA-based alpha- and beta-chain genes under the control of heterologous regulatory elements. Immunol. Cell. Biol. 1998; 76:34–40. [PubMed: 9553774]
46. Scollay RG, Butcher EC, Weissman IL. Thymus cell migration. Quantitative aspects of cellular traffic from the thymus to the periphery in mice. Eur. J. Immunol. 1980; 10:210–218. [PubMed: 7379836]
47. Hataye J, Moon JJ, Khoruts A, Reilly C, Jenkins MK. Naive and memory CD4+ T cell survival controlled by clonal abundance. Science. 2006; 312:114–116. [PubMed: 16513943]

48. Huseby ES, White J, Crawford F, Vass T, Becker D, Pinilla C, Marrack P, Kappler JW. How the T cell repertoire becomes peptide and MHC specific. Cell. 2005; 122:247–260. [PubMed: 16051149]

49. Kosmrlj A, Read EL, Qi Y, Allen TM, Altfeld M, Deeks SG, Pereyra F, Carrington M, Walker BD, Chakraborty AK. Effects of thymic selection of the T-cell repertoire on HLA class I-associated control of HIV infection. Nature. 2010; 465:350–354. [PubMed: 20445539]

50. Gallivan JP, Dougherty DA. Cation-pi interactions in structural biology. Proc. Natl. Acad. Sci. U S A. 1999; 96:9459–9464. [PubMed: 10449714]

51. Chen JL, Stewart-Jones G, Bossi G, Lissin NM, Wooldridge L, Choi EM, Held G, Dunbar PR, Esnouf RM, Sami M, Boulter JM, Rizkallah P, Renner C, Sewell A, van der Merwe PA, Jakobsen BK, Griffiths G, Jones EY, Cerundolo V. Structural and kinetic basis for heightened immunogenicity of T cell vaccines. J. Exp. Med. 2005; 201:1243–1255. [PubMed: 15837811]

52. Turner SJ, Doherty PC, McCluskey J, Rossjohn J. Structural determinants of T-cell receptor bias in immunity. Nat. Rev. Immunol. 2006; 6:883–894. [PubMed: 17110956]

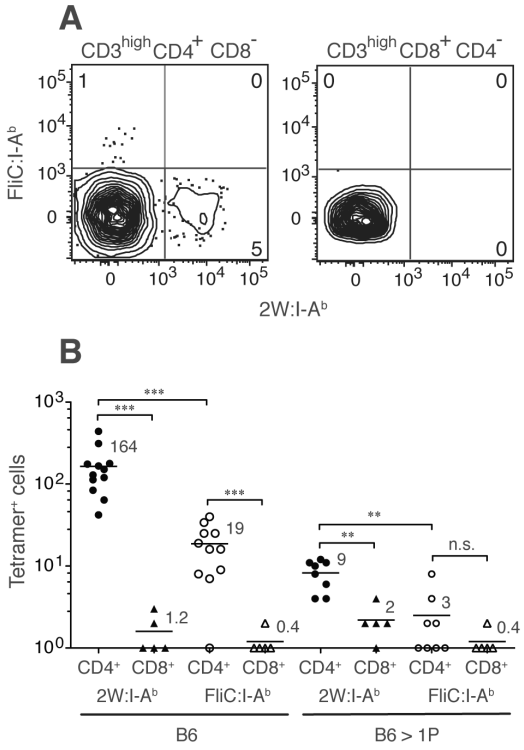

Figure 1.

Perturbation of positive selection affects the sizes of naïve CD4$^+$ T cell populations. **A**, Contour plots of FliC:I-A^b tetramer versus 2W:I-A^b tetramer staining for CD3^{high} CD4$^+$ CD8$^-$ (left) or CD8$^+$CD4$^-$ (right) thymocytes from tetramer-enriched thymus samples from naïve B6 mice. Numbers on plots indicate the percentage of cells in each quadrant. **B**, Total CD3^{high} CD4$^+$ CD8$^-$ or CD8$^+$ CD4$^-$ 2W:I-A^{b+} (filled symbols), or FliC:I-A^{b+} (open symbols) cells from thymus samples of individual B6 controls, B6 > *H2-DMa*$^{-/-}$ chimeras, or B6 > Y-Ae (B6 > 1P) chimeras. Numbers above each group represent its mean value. *** *P*-value < 0.001; ** *P*-value ≤ 0.01 (unpaired two-tailed Student's *t*-test). Data are representative of five independent experiments.

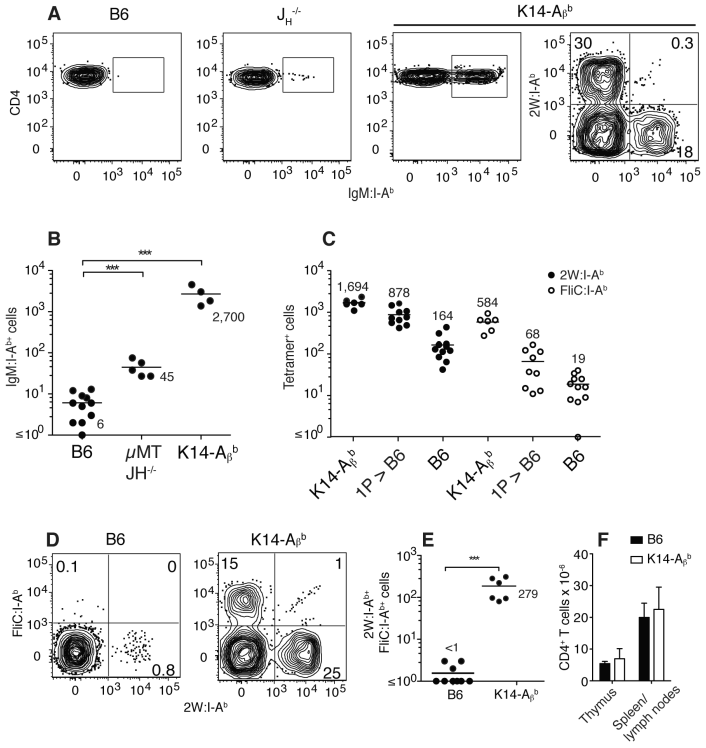

Figure 2.

Perturbation of negative selection affects the sizes of naïve CD4$^+$ T cell populations. **A,** Contour plots of CD4 versus IgM:I-A^b tetramer staining for CD3^{high} CD4$^+$ CD8$^-$ thymocytes from tetramer-enriched thymus samples from naïve B6, *JH*$^{-/-}$ or K14-A$_\beta^b$ mice, or 2W:I-A^b tetramer versus IgM:I-A^b tetramer staining for CD3^{high} CD4$^+$ thymocytes from tetramer-enriched thymus samples from naïve K14-A$_\beta^b$ mice. **B**, Total CD3^{high} CD4$^+$ IgM:I-A^{b+} cells from thymus samples of individual B6, μMT or *JH*$^{-/-}$, or K14-A$_b^b$ mice. **C**, Total CD3^{high} CD4$^+$ CD8$^-$ 2W:I-A^{b+} b (filled circles) or FliC:I-A^{b+} (open circles) thymocytes from individual B6, K14-A$_\beta^b$, or *H2-DMa*$^{-/-}$ > B6 or Y-Ae > B6 (1P > B6) chimeric mice. **D**, Contour plots of FliC:I-A^b versus 2W:I-A^b tetramer staining for CD3$^+$ CD44^{low} CD4$^+$ T cells from tetramer-enriched spleen and lymph node samples from naïve B6 (left) or K14-A$_\beta^b$ mice (right). **E**, Total CD4$^+$ cells from spleen and lymph nodes of individual B6 or K14-A_b^b mice that bound both FliC:I-A^b and 2W:I-A^b tetramers. **F**, Mean total CD4$^+$ cells (± SD) in the thymus or spleen and lymph nodes of B6 or K14-A_b^b mice. Numbers on the plots in **A** and **D** indicate the percentage of cells in each quadrant. Numbers on the graphs in **B**, **C**, and **E** represent mean values and are indicated as horizontal bars. *** *P*-value < 0.001. Data are from three independent experiments.

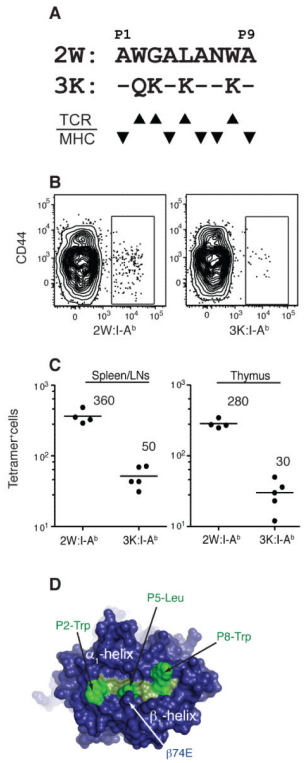

Figure 3.

The large size of the 2W:I-A^b-specific population is associated with its specific TCR contact residues. **A**, I-A^b-binding nonamers for 2W and 3K peptides with TCR and I-A^b contacts indicated. **B**, Contour plots of CD44 versus 2W:I-A^b (left) or 3K:I-A^b (right) tetramer staining for CD4$^+$ T cells from tetramer-enriched spleen and lymph node samples from naïve B6 mice. **C**, Total CD4$^+$ 2W:I-A^{b+} or 3K:I-A^{b+} cells from spleen and lymph nodes (left) or thymus (right) samples of individual B6 mice. Mean values for each group are indicated as horizontal bars and numerically for each set of values. Data are from at least three independent experiments. **D**, Model structure of 2W:I-A^b (top view). The 2W peptide is in green, while the I-A^b molecule is in blue. The structure is positioned with the peptide N terminus on the left, the I-A^b β_1-helix at the bottom and the α_1-helix at the top. Black arrows indicate the predicted TCR contact residue side chains. Residue I-A^b β74E that partly occludes residue P5L of the 2W peptide is indicated by a white arrow.

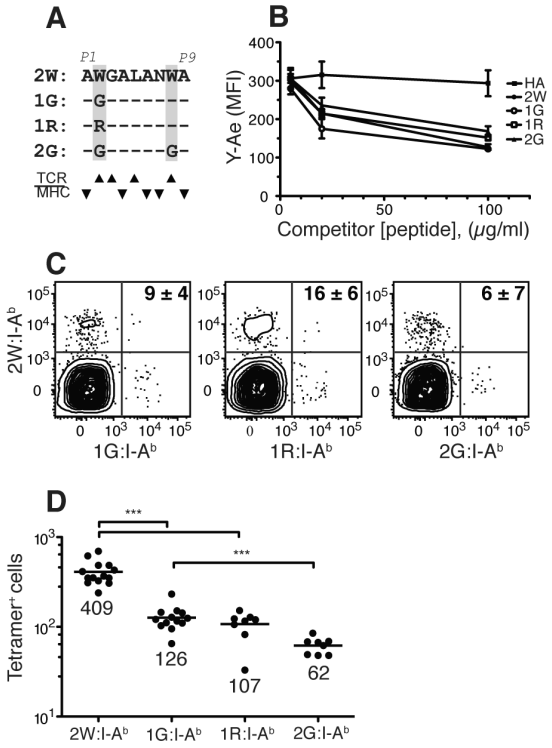

Figure 4.

Tryptophan residues at TCR contact P2 and P8 contribute to the large size of the 2W:I-A^b-specific population. **A**, I-A^b-binding nonamers for 2W and its variant 1G, 1R and 2G peptides. **B**, Normalized mean fluorescence intensities (MFI) of anti-Eα52-68:I-A^b (Y-Ae) staining from B220$^+$ *H2-DMa*$^{-/-}$ spleen cells after incubation with the Eα52-68 peptide plus the indicated concentrations of the control $HA_{307-319}$ peptide (filled squares), 2W (filled circles), 1G (open circles), 1R (open squares) or 2G (triangles) peptides. A reduction in Y-Ae staining indicated that the test peptide out competed the Ea_{52-68} peptide for binding to I-A^b. **C**, Contour plots of 2W:I-A^b versus 1G:I-A^b, 1R:I-A^b or 2G:I-A^b tetramer staining for CD4$^+$ T cells from tetramer-enriched spleen and lymph node samples from naïve individual B6 mice. Numbers in the upper right quadrant of each plot represented the mean percent (± SD, n =3) of the 1G:I-A^{b+}, 1R:I-A^{b+} or 2G:I-A^{b+} populations that were also 2W:I-A^{b+}. **D**, Total CD4$^+$ 2W:I-A^{b+}, 1G:I-A^{b+}, 1R:I-A^{b+} or 2G:I-A^{b+} T cells from spleen and lymph node samples of individual B6 mice. Mean values for each group are indicated as horizontal bars and numerically for each set of values. *** P-value < 0.001. Data are from at least three independent experiments.

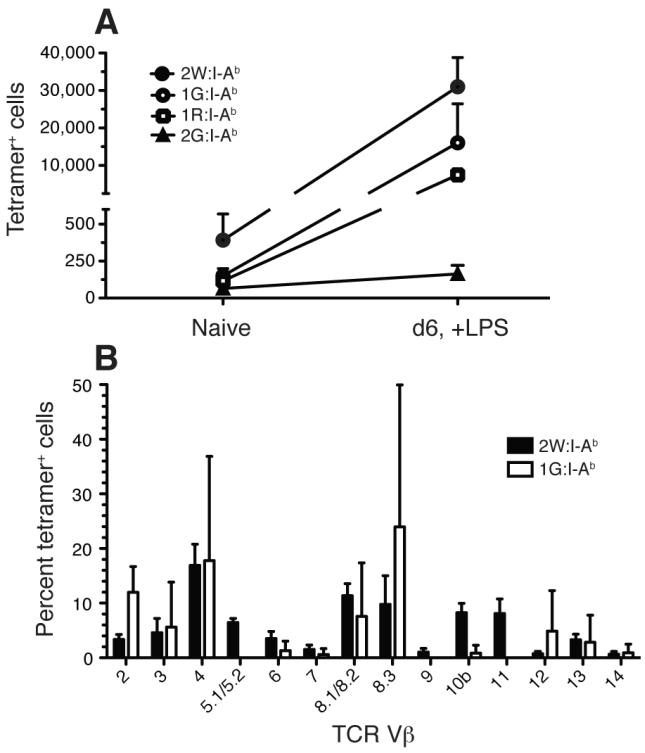

Figure 5.

The 2W:I-A^b-specific population is larger in size and more diverse in TCR Vβ usage than those specific for 1G:I-A^b. **A**, Mean CD4$^+$ 2W:I-A^{b+} (filled circles), 1G:I-A^{b+} (open circles), 1R:I-A^{b+} (squares) or 2G:I-A^{b+} (triangles) cells (± SD, n = 3-5 per specificity) from spleen and lymph node samples of individual B6 mice 6 days after intravenous injection of the relevant peptide plus LPS. **B**, TCR Vβ usage by CD4$^+$ 2W:I-A^{b+} (filled bars) or 1G:I-A^{b+} (open bars) cells from spleen and lymph node samples of B6 mice 6 days after intravenous injection with relevant peptide plus LPS. Data are mean values ± SD from 2 mice per group from two independent experiments.

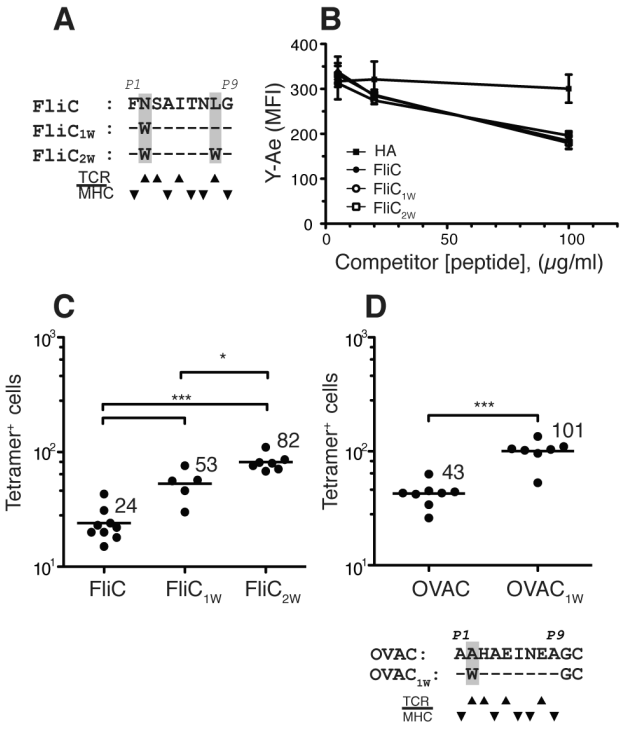

Figure 6.

Tryptophan residues at TCR contact P2 and P8 increase the sizes of other peptide:I-A^b-specific populations. **A**, I-A^b-binding nonamers for FliC and its variants $FliC_{1W}$ and $FliC_{2W}$. **B**, Normalized MFI of anti-$E\alpha_{52\text{-}68}$:I-A^b (Y-Ae) staining of $B220^+$ *H2-DMa*$^{-/-}$ spleen cells after incubation with the $E\alpha_{52\text{-}68}$ peptide plus the indicated concentrations of the control $HA_{307\text{-}319}$ peptide or FliC variant peptides. **C,** Total $CD4^+$ FliC:I-A^{b+}, $FliC_{1W}$:I-A^{b+}, or $FliC_{2W}$:I-A^{b+} cells from spleen and lymph node samples of individual B6 mice. **D**, Total $CD4^+$ OVAC:I-A^{b+} or $OVAC_{1W}$:I-A^{b+} cells from spleen and lymph node samples of individual B6 mice. I-A^b-binding nonamers for OVAC and $OVAC_{1W}$ are shown below the figure. The cysteine residues at the C termini of OVAC and $OVAC_{1W}$ used for disulfide linkage with the cysteine residues at position 72 of the I-A^b alpha chain are also shown. Mean values for each group are indicated as horizontal bars and numerically under each set of values. *** *P*-value < 0.001; * *P*-value < 0.05. Data are from at least three independent experiments.